

RING CURRENT - PLASMASPHERE COUPLING THROUGH COULOMB COLLISIONS

M.-C. Fok, P. D. Craven, T. E. Moore

Space Sciences Laboratory, NASA Marshall Space Flight Center, Huntsville, AL 35812

and

P. G. Richards

CSPAR, The University of Alabama in Huntsville, Huntsville, AL 35899

Abstract In the ring current-plasmasphere region, two plasma populations interact with each other via multiple processes, such as Coulomb collisions and wave-particle interactions. In this paper, the consequences of coupling between ring current ions and the plasmasphere through Coulomb collisions are examined. A kinetic **R**ing **C**urrent-**A**tmosphere Interaction **M**odel (RAM) has been used to solve the temporal evolution of the ring current ion distribution and obtain the instantaneous ring current heating to the plasmasphere through Coulomb collisions. A buildup of low-energy (< 1 keV) ion population is found as a result of energy degradation of ring current ions in a background of thermal plasma. The "drift-holes" in the ring current ion energy spectra are also somewhat smoothed out by Coulomb interactions. Energy transferred from ring current ions to the plasmasphere is a source of plasma heating and results in enhanced plasma temperatures at high altitudes. The ion temperatures calculated from the FLIP (Field Line Interhemispheric Plasma) model, taking into account the additional heat source from the ring current, appear to be consistent with the enhanced ion temperatures observed in the high altitude regime.

Introduction

In the region of overlap between the ring current and the plasmasphere, two plasma populations interact with each other via multiple processes, such as wave-particle interactions and Coulomb collisions. Energy of the ring current ions is a source of free energy to excite plasma waves. This energy, in turn, will be redistributed amongst the thermal and energetic populations as the plasma waves undergo damping. Energy contained in the ring current can also be transferred to the plasmasphere through Coulomb collisions. Previous studies on the interactions between the ring current and the plasmasphere and the effects on both plasma populations are summarized in the review of *Kozyra and Nagy* [1991].

In this paper, results on the coupling between the ring current ions and the plasmasphere through Coulomb collisions are presented. Hereafter, ring current ions are designated as energetic plasma and the plasma (ions and electrons) in the plasmasphere as thermal plasma. When energetic ions move through a background of thermal plasma in the plasmasphere, they experience energy loss but very small angular deflection. Since the energy transfer rate is maximum when the velocity of the energetic ions and that of the thermal species are comparable (function G in Eq. (21) of *Fok et al.*, 1993), most of the energy received by the thermal plasma goes to the electrons. However the conductivity of thermal ions is about one fortieth that of thermal electrons. A small amount of heating from the ring current may produce enhanced ion temperatures comparable to, or higher, than the electron temperatures in the plasmasphere. Interactions with the plasmasphere also have a significant effect on the energetic population as it undergoes energy degradation.

A previously established **Ring current-Atmosphere interaction Model (RAM)** [Fok *et al.*, 1993, 1995] is used to study the coupling between ring current ions and the plasmasphere. RAM is a kinetic model solving the temporal evolution of ring current ion phase space density, considering drift motion, charge exchange with the hydrogen geocorona, and Coulomb interactions with the plasmasphere. The instantaneous heating rate to the plasmasphere is also calculated. The response of the plasmasphere to the additional heating by the ring current is investigated using the FLIP (Field Line Interhemispheric Plasma) model [Richards and Torr, 1985; Torr *et al.*, 1990]. For comparison, plasmaspheric ion temperatures are calculated from FLIP, with and without heating from the ring current.

The Model: RAM

The temporal and spatial variations of the phase space density, f_s , of ring current ion species, s , can be obtained by solving the following kinetic equation, considering drift motion, charge exchange with the neutral hydrogen geocorona, and Coulomb collisions with the plasmasphere

$$\frac{\partial \bar{f}_s}{\partial t} + \langle \dot{R}_0 \rangle \frac{\partial \bar{f}_s}{\partial R_0} + \langle \dot{\phi} \rangle \frac{\partial \bar{f}_s}{\partial \phi} = -\nu \sigma_s \langle n_H \rangle \bar{f}_s + \frac{1}{M^{1/2}} \frac{\partial}{\partial M} \left(\langle \dot{M} \rangle M^{1/2} \bar{f}_s \right) \quad (1)$$

where R_0 is the radial distance at the equator, ϕ is the magnetic local time, M is the magnetic moment, and \bar{f}_s is the average f_s along the field line between mirror points. Since the bounce period of ions in the ring current energy range is much shorter than the decay lifetimes, f_s is assumed to be constant along the field line and thus \bar{f}_s can be replaced by the distribution function at the equator. $\langle x \rangle$ is the bounce-averaged value of quantity x .

For the collisional terms in (1), σ_s is the cross section for charge exchange of species s with neutral hydrogen, and n_H is the hydrogen density. \dot{M} is the rate of change of magnetic moment due to the Coulomb drag from the plasmasphere and it is proportional to the background plasma density. A time-dependent, two-dimensional plasmasphere model of *Rasmussen et al.* [1993] is used to calculate \dot{M} . This is the unique feature of RAM, which incorporates a time-dependent plasmasphere model to calculate effects of Coulomb collisions between the energetic and the thermal population. The instantaneous heating rate from the ring current to the plasmaspheric species p is given by

$$Q_p = \frac{1}{\Delta t} \sum_s \left(\int \Delta f_s \frac{1}{2} m v^2 d^3 v \right) \quad (2)$$

where Δf_s is the change of f_s in Δt due to Coulomb collisions with species p . More details of RAM can be found in *Fok et al.* [1993, 1995].

Coulomb Collision Effects on the Energetics

As a result of frictional forces exerted on the ring current ions by the background plasma in the plasmasphere, the energy spectra of the energetic ions shift toward low energies. This effect on the energetic ion distribution is clearly illustrated in Figure 1. Given an initial H⁺ (Figure 1a) and O⁺ (Figure 1b) ion distribution, peaking at 10 keV (top panel) and 40 keV (middle panel) in a background thermal (1 eV) plasma with density of 2000 cm⁻³, the temporal evolution of these distributions is calculated taking into account only Coulomb interactions. The variation in rate of energy loss as a function of ion energy (bottom panel) is provided as a convenient reference. Energy loss rate in energy space peaks at 4 keV for H⁺ (bottom panel, Figure 1a) and at 50 keV for O⁺ (bottom panel, Figure 1b). Ions will be removed rapidly from regions of peak energy loss rate and will build up in regions of lower energy loss rate. The effect is dramatically

illustrated in the top panels of Figure 1a and 1b. A low-energy (< 1 keV) flux of H^+ builds up after 12 hours as a result of energy loss by the "10-keV" H^+ . However, this low-energy population diminishes after 2 days of interaction. Low-energy O^+ fluxes build up more slowly. They only reach values comparable to the peak low-energy H^+ fluxes after 2 days have elapsed. In contrast the peak low-energy H^+ fluxes appear after 1 day of decay. This buildup of low-energy ions is also predicted by the model of *Jordanova et al.* [1994].

The buildup of low-energy ions from a 40-keV initial ion distribution is much less dramatic (middle panels, Figures 1a and 1b). The 40-keV peak in the H^+ flux occurs in a region of increasing energy loss rate as ions degrade in energy. Ions move from a region of slower to faster energy loss (toward the left in the middle panel, Figure 1a). As a consequence, the H^+ distribution is eroded, with only a weak buildup at the lowest energies. The 40-keV peak in the O^+ flux (middle panel, Figure 1b), occurs in a region of nearly constant energy loss rate. For this case, the O^+ peak is convected in energy space, almost without change in amplitude or shape, to lower energies. Eventually, as time increases beyond 2 days, a flux buildup at the low energies is expected to occur.

The buildup of the low-energy ion population predicted above is reproduced when calculating the whole phase space densities of ring current ions during the recovery of a model storm of moderate intensity. The initial (when the recovery starts) conditions of the model storm are taken from the average stormtime spectra reported by *Kistler et al.* [1989]. The Kp value is assumed to be 6 initially and decreases at a constant rate in 15 hours to the post recovery value of 1 (top panel, Plate 1). The 10–500 eV fluxes derived from the ring current H^+ and O^+ as a function of elapsed time are calculated. Plate 1 shows the initial fluxes, and the fluxes at 12 hours and 2 days after the main phase of the storm. For both ions, the maximum fluxes are initially located in the region of L between 3–4, at midnight local time (Plate 1a). The initial fluxes on the dayside are assumed to be

0. Twelve hours later (Plate 1b), fluxes of the same order of magnitude or higher than the initial peak are found at a lower L shell ($L \sim 2.5$). Particles which have open drift paths move toward the upper spatial boundary of the model and are lost. Therefore, the longest-lived fluxes are confined to a range of L values from about 2.5 to 3.5, where drift paths are closed.

After 2 days of recovery (Plate 1c), there is an order of magnitude decrease in the maximum H^+ flux. The maximum flux at this time has moved outward to $L \sim 4$. The temporal history of the low-energy O^+ flux is much different than that of the low-energy H^+ ions. The maximum O^+ flux in the energy range 10–500 eV is located at $L \sim 2.75$, but does not appear until 2 days into the recovery phase. The different times for buildup and disappearance of each ion species in this energy range (10–500 eV) are consistent with the simulations shown in Figure 1 and can be explained by their different rates of energy loss to the plasmasphere. After the low-energy H^+ is built up, it will be lost by energy degradation in a few hours. It takes about 1 day for low-energy O^+ to be formed from high-energy particles, as a result of its comparatively long Coulomb lifetime; therefore, it lasts for a few days.

The other effect on the energetic ions due to Coulomb collisions with the plasmasphere is the shallower minimum in the energy distribution. Dips or sharp drop-offs in the ion energy spectra for $1 \leq E \leq 10$ keV are consistent features in observations [McIlwain, 1972; Lennartsson *et al.*, 1981; Kistler *et al.*, 1989]. Corotation dominates the motion of low-energy ions, whereas high-energy ions drift westward due to the gradient and curvature in the magnetic field. Ions of intermediate energies experience eastward and westward drifts that are similar in magnitude, resulting in very slow drift velocity. The hole in the energy spectra corresponds to particles at these energies which have either not yet reached the observation point or which have experienced significant losses during their slow drift to the observation point. Cornwall [1972] and Spjeldvik [1977] found that Coulomb collisions with the plasmasphere made the dips caused by

drift motion shallower when they calculated the equilibrium density structure of the magnetosphere ions.

In order to see the effect of Coulomb drag on the shape of the "drift hole", ion energy spectra are calculated for different cases: (1) considering only drift motion, (2) drifts plus charge exchange loss, and (3) same as (2) except Coulomb collisions are also included. Figure 2 shows these test results of H^+ at two locations. At $L = 2.5$ (Figure 2a), the inclusion of Coulomb collisions results in a slight reduction of the distribution function at high energies (> 50 keV). However, a low-energy (< 1 keV) ion population is formed by the energy degradation of high-energy ions. Coulomb collisions also make the dip caused by drift motion shallower. At L values outside the plasmapause ($L = 4$, Figure 2b) the Coulomb collision effects are much weaker. However, the partial filling-in of the drift hole is still observed. *Kistler et al.* [1989] only considered drifts and charge exchange loss of ring current ions. They found that at low energies, the observed fluxes were higher than predicted and that the dips in some of their modeled spectra were deeper than the measurements. The inclusion of Coulomb collisions in our model leads to a better agreement with observations, especially at low energies. Coulomb collisions also have pronounced effects on the low-energy distribution of ring current He^+ and O^+ ions.

Ring Current Heating of the Plasmasphere

Under the assumptions of uniform plasmasphere density along field lines and constant phase space density between mirror points for the ring current ions, RAM is able to calculate the instantaneous volume heating rate (at a given local time, latitude, and altitude) to the plasmasphere that is a consequence of collisions between thermal ions and ring current ions. Only heating to the thermal ions is discussed in this work. In order to see what ring current species and energies contribute to the heating of thermal ions, the rate of change of the energy of energetic ions moving through a background thermal ion

gas is calculated and plotted in Figure 3 as a function of the energy of the incoming ions. As shown in the figure, low-energy (< 10 keV) O^+ is the main source of heating to the thermal ions via Coulomb interactions, unless the ring current is overwhelmingly dominated by H^+ . The energy transfer rates are fairly constant over a wide range of thermal ion temperature observed in the plasmasphere ($0.2\text{--}2$ eV) [Comfort *et al.*, 1988]. In contrast, the efficiency of energy transfer to the thermal electrons is sensitive to the thermal electron temperature.

We calculate the volume heating rate to the thermal ions in the plasmasphere during the recovery phase of a modeled major storm similar to that which occurred in early February 1986. The initial distribution of ring current ions (at the minimum *Dst*) is taken from AMPTE/CCE spacecraft observations spanning the *L* value range $L = 2.25$ to 6.75 . Ion fluxes at energies of 10 eV to 1.52 keV, which is the lowest energy bin of CCE measurement, are estimated by linear extrapolation. The simulated temporal evolution of the ring current ions during the recovery of this storm is presented in Fok *et al.* [1995]. In general, the calculated ion fluxes are consistent with observations, except for H^+ fluxes at tens of keV, which are always over-estimated. However this discrepancy has only a small effect on the plasmaspheric heating rate because the main contribution of heating comes from the ring current O^+ ions. Plate 2 shows the volume heating rate to the thermal ions at the equator (left panels) and the noon-midnight meridian (right panels) at (a) 2 and (b) 52 hours after the start of the recovery phase, together with the corresponding *Kp* values. At 2 hours, the maximum heating rate is on the order of 1 eVcm⁻³s⁻¹ and is located at *L* shell of 2 to 2.5, with local time extending from midnight to dawn. The region of high heating rate corresponds to the location of peak density of low-energy (< 10 keV) ring current ions during the early recovery. This region of high heating rate drifts eastward and reaches noon in the next few hours as the low-energy ring current ions corotate. The isocontours of heating rate at *L* shells larger than 3 roughly follow the thermal density calculated from the model of Rasmussen *et al.* [1993]. The

plasmasphere bulge located between noon and dusk during this active period can be inferred in the equatorial view of Plate 2a. The meridian view shows that the heating rate peaks at the equator near the inner edge of the ring current and is fairly uniform along field lines at high L shells. The localized heating near the Earth is a consequence of ring current ions which have an anisotropic pitch-angle distribution (peaks at 90°) caused by strong charge exchange loss at low L shells. The distribution of the heating rate is a result of the combined effect of the densities of the source (ring current ions with energy less than 10 keV) and the sink (thermal ions).

In late recovery (Plate 2b), isocontours of heating rate expand and fall off with L smoothly as a result of the refilling of the plasmasphere during the storm recovery. The high heating rate (on the order of $1 \text{ eVcm}^{-3}\text{s}^{-1}$), which is seen at $L < 2.5$ at 2 hours, is diminished due to the charge exchange losses of low-energy ($< 10 \text{ keV}$) ions at that location. In contrast, the heating rates at high L 's are higher at late recovery than at early recovery. In the meridian view, the peak heating rate at the equator is more pronounced and extends to higher L shells as a consequence of strong ring current pitch-angle anisotropy during late recovery of the storm [Fok *et al.*, 1995].

Plasmaspheric Response to the Heating from Ring Current

The energy loss of the ring current from Coulomb decay is small compared with that of the charge exchange loss. However, this small amount of energy may be a significant heat source to the thermal plasma in the plasmasphere. The energy received by the thermal plasma in the plasmasphere is, in turn, conducted down along field lines to the ionosphere and produces observable signatures. A number of works have shown that the energy transferred to the plasmasphere through Coulomb collisions with the ring current ions is responsible for the enhanced plasmaspheric temperature and resulting

ionospheric electron temperature peaks and associated stable auroral red (SAR) arc emissions [Cole, 1965; Kozyra *et al.*, 1987; Chandler *et al.*, 1988; Fok *et al.*, 1993].

In order to see the plasmaspheric response to the heating from the energetic ions, the thermal ion temperatures are calculated using the RAM-generated heat source for the February 1986 storm as input to the FLIP model. The volume heating rate calculated from RAM is scaled by the ratio of plasmaspheric densities obtained from the model of Rasmussen *et al.* [1993] and FLIP. We modified the standard FLIP model slightly in order to accommodate direct ion heating from the ring current source. Otherwise the model is the same as described by Richards and Torr [1985], and Torr *et al.* [1990]. FLIP, as used here, solves the continuity, momentum, and energy equations along the flux tube from 120 km in one hemisphere to 120 km in the conjugate hemisphere. All ion species are assumed to have the same temperature, but are different from those of thermal electrons. Since the ring current heating to the thermal electrons depends on the thermal electron temperature, RAM and FLIP have to be run interactively in order to have consistent results. Because of this, heating to the thermal electrons and the resulting electron temperature enhancements are excluded in the present study. This problem will be addressed in our future work.

The equatorial ion temperatures calculated from FLIP for $L = 2$ and 4 as a function of elapsed time from the beginning of the recovery phase are plotted in Figure 4. Because the flux tube corotates, the local time changes with the elapsed time. Local time is also shown in Figure 4. The storm starts at 0 hour recovery time (RT) and decays to quiet time rates at 60 hours RT. The insert in Plate 2 shows the Kp history. Results with and without heating from ring current are displayed. As shown in Figure 4, at $L = 2$, including the ring current heat source greatly increases the ion temperature from the night side to dawn but has almost no effect from noon to dusk. The local time asymmetry of the magnetospheric heat source enhances the diurnal variation in the ion temperature

and causes the daily minimum temperature to shift from the nightside to dusk. The decrease in the ring current heating at dusk, at $L = 2$, is a result of low-energy (< 10 keV) ring current ions being significantly removed by charge exchange before reaching the dusk side. The high heating rate at $L = 2$ fades away as the storm recovery proceeds (Plate 2). The maximum ion temperature thus decreases in the same manner. At $L = 4$, the effects of the ring current heating of the thermal ions are obvious at all local times because the ring current is fairly constant with local time at this L value (Plate 2). Also the ion temperature enhancement persists during the long recovery since the source experiences few losses at $L = 4$ and low-energy ring current ions are continuously replenished from the tail.

The altitude profiles of ion temperature at $L = 2$ and 4, on the morning and evening side, at different elapsed times during the storm recovery as calculated from FLIP are plotted in Figure 5. In all cases, heating from the ring current increases the ion temperature at altitudes above the heat sink due to the neutral atmosphere, about 500 km. Once again the temperature at $L = 2$, 0900 LT, increases rapidly during the early recovery phase and then gradually returns to the quiet time level. On the other hand, T_i at $L = 4$ is increasing throughout the recovery until $t \sim 50$ hours after which it decreases. There is a two- to five-fold increase in temperature compared with no heating from ring current except at $L = 2$, 2200 LT, where the heating rate is low for this particular storm (Plate 2). For comparison, the mean DE 1/RIMS H^+ temperatures during October and November of 1981 [Comfort *et al.*, 1988] are also shown. In general, heating from the ring current can more than account for the ion temperature observed. In particular, the high temperature ($T_i \sim 14000$ K) near dawn at $L = 2$ predicted by this study has not been observed. The over-estimation of the low-energy (< 1.52 keV) ion fluxes by linear extrapolation may be responsible for producing this high ion temperature. If the initial low-energy (< 1.52 keV) ion fluxes are set equal to the 1.52 keV flux measured by AMPTE/CCE, the resulting heating rates to the thermal ions at $L < 2.5$ are approximately an order of

magnitude lower than those presented in Plate 2. The corresponding equatorial ion temperature near dawn at $L = 2$ only reaches a peak value of 4700 K during the early recovery. Since the ring current ion energy spectra become flat in shape at low energies for $L > 3.5$ (Figure 2, *Fok et al.*, 1995), the way of extrapolating initial ion fluxes down to 10 eV does not much affect the plasmaspheric heating and the resulting ion temperature for $L > 3.5$. Accurate modeling of the energy range below 1.52 keV will require measurements in that energy range as initial conditions.

In contrast to the predicted high temperature on the dawn side at $L = 2$, the ion temperature at $L = 2$, 2200 LT increases by less than 1000 K with the heating from the energetic ions (upper right panel, Figure 5). However, if the heating of plasmaspheric electrons from the ring current is considered, the enhanced electron temperature is expected to raise the ion temperature to a value closer to measurements. Although we are comparing the simulated results with the observed temperature averaged over the period of October to November 1981, in which geomagnetic activity did not reach a level as high as the February 1986 storm, we have clearly shown that the enhanced ion temperature in the plasmasphere can be explained with the heating from a magnetospheric source. Moreover, the relationship between the ion temperature and geomagnetic activity is surely not trivial. It may depend on the instantaneous activity level, perhaps even the past history of geomagnetic activity, also on the phase of the storm at which the measurements are made.

Discussion and Summary

The observed temperature enhancements at high altitudes indicate the existence of a magnetospheric heat source [*Horwitz and Chappell*, 1979; *Farrugia et al.*, 1989; *Craven et al.*, 1991]. Previous studies [*Chandler et al.*, 1988; *Fok et al.*, 1993] and this

study suggest that energy transferred from the ring current ions to the plasmasphere via Coulomb interactions is a significant heat source to power the plasmaspheric temperatures to the observed levels and can produce significant diurnal variations in the thermal plasma temperature. In the future, heating of thermal electrons in the plasmasphere from ring current ions will also be considered in order to have a better picture of plasmaspheric heating. Other mechanisms, such as wave-particle interactions, may also contribute to the plasmaspheric heating. Various kinds of plasma waves have been observed [cf., *Korth et al.*, 1984; *LaBelle et al.*, 1988] and theoretical studies suggest that the unstable plasma waves heat the thermal population [*Roth et al.*, 1990; *Gorbachev et al.*, 1992]. Although wave-particle interactions are presently not included in RAM, RAM can serve as a baseline model to distinguish or separate the wave effects on the plasmaspheric heating.

The role of Coulomb collisions on the ring current dynamics sometimes does not receive much attention. However, we found that ring current Coulomb interactions with the plasmasphere are important processes for both energetic and thermal populations. The buildup of a low-energy ion population, predicted by RAM, may be a source of the low-energy ions observed in the inner magnetosphere [*Lennartsson and Sharp*, 1982; *Shelley et al.*, 1985].

In summary, we found the following consequences of the ring current-plasmasphere coupling through Coulomb collisions:

- (1) A low-energy (< 1 keV) ion population is formed as ring current ions degrade in energy.
- (2) Dips in ring current ion energy spectra caused by drift motion are somewhat smoothed out by Coulomb drag.
- (3) Energy transferred from ring current ions to the plasmasphere is a significant heat source for the thermal plasma at high altitudes.

Acknowledgement This work was performed while one of us, M.-C. Fok, held a National Research Council-Marshall Space Flight Center Research Associateship. Other work at MSFC was supported by the NASA Space Physics Division under UPN 432-20-00. Support at the University of Alabama was from NASA grant NAGW 996.

References

- Chandler, M. O., J. U. Kozyra, J. L. Horwitz, R. H. Comfort, and L. H. Brace, Modeling of the thermal plasma in the outer plasmasphere - A magnetospheric heat source, in *Modeling Magnetospheric Plasma, Geophys. Monogr. Ser., vol. 44*, edited by T. E. Moore and J. H. Waite Jr., pp. 101-105, AGU, Washington, D. C., 1988.
- Cole, K. D., Stable auroral red arc, sinks for energy of Dst main phase, *J. Geophys. Res.*, *70*, 1689-1706, 1965.
- Comfort, R. H., I. T. Newberry, and C. R. Chappell, Preliminary statistical survey of plasmaspheric ion properties from observations by DE 1/RIMS, in *Modeling Magnetospheric Plasma, Geophys. Monogr. Ser., vol. 44*, edited by T. E. Moore and J. H. Waite Jr., pp. 107-114, AGU, Washington, D. C., 1988.
- Cornwall, J. M., Radial diffusion of ionized helium and protons: A probe for magnetospheric dynamics, *J. Geophys. Res.*, *77*, 1756-1770, 1972.
- Craven, P. D., R. H. Comfort, D. L. Gallagher, and R. West, A study of the statistical behavior of ion temperatures from DE 1/RIMS, in *Modeling Magnetospheric Plasma Processes, Geophys. Monogr. Ser., vol. 62*, edited by G. R. Wilson, pp. 173-182, AGU, Washington, D. C., 1991.

- Farrugia, C. J., D. J. Young, J. Geiss, and H. Balsiger, The composition, temperature, and density structure of cold ions in the quiet terrestrial plasmasphere: GEOS 1 results, *J. Geophys. Res.*, *94*, 11,865-11,891, 1989.
- Fok, M.-C., J. U. Kozyra, A. F. Nagy, C. E. Rasmussen, and G. V. Khazanov, Decay of equatorial ring current ions and associated aeronomical consequences, *J. Geophys. Res.*, *98*, 19,381-19,393, 1993.
- Fok, M.-C., T. E. Moore, J. U. Kozyra, G. C. Ho, and D. C. Hamilton, Three-dimensional ring current decay model, *J. Geophys. Res.*, in press, 1995.
- Gorbachev, O. A., G. V. Khazanov, K. V. Gamayunov, and E. N. Krivorutsky, A theoretical model for the ring current interaction with the Earth's plasmasphere, *Planet. Space Sci.*, *40*, 859-872, 1992.
- Horwitz, J. L., and C. R. Chappell, Observations of warm plasma in the dayside plasma trough at geosynchronous, *J. Geophys. Res.*, *84*, 7075-7090, 1979.
- Jordanova, V. K., J. U. Kozyra, G. V. Khazanov, A. F. Nagy, C. E. Rasmussen, and M.-C. Fok, A bounce-averaged kinetic model of the ring current ion population, *Geophys. Res. Lett.*, *21*, 2785-2788, 1994.
- Kistler, L. M., F. M. Ipavich, D. C. Hamilton, G. Gloeckler, B. Wilken, G. Kremser, and W. Stüdemann, Energy spectra of the major ion species in the ring current during geomagnetic storms, *J. Geophys. Res.*, *94*, 3579-3599, 1989.
- Korth, A., G. Kremser, S. Perraut, and A. Roux, Interaction of particles with ion cyclotron waves and magnetosonic waves. Observations from GEOS 1 and GEOS 2, *Planet. Space Sci.*, *32*, 1393-1406, 1984.
- Kozyra, J. U., and A. F. Nagy, Ring current decay-coupling of ring current energy into the thermosphere/ionosphere system, *J. Geomag. Geoelectr.*, *43*, 285-297, 1991.
- Kozyra, J. U., E. G. Shelley, R. H. Comfort, L. H. Brace, T. E. Cravens, and A. F. Nagy, The role of ring current O⁺ in the formation of stable auroral red arcs, *J. Geophys. Res.*, *92*, 7487-7502, 1987.

- LaBelle, J., R. A. Treumann, W. Baumjohann, G. Haerendel, N. Sckopke, G. Paschmann, and H. Luhr, The duskside plasmopause/ring current interface: Convection and plasma wave observations, *J. Geophys. Res.*, *93*, 2573-2590, 1988.
- Lennartsson, W., and R. D. Sharp, A comparison of the 0.1–17 keV/e ion composition in the near equatorial magnetosphere between quiet and disturbed conditions, *J. Geophys. Res.*, *87*, 6109-6120, 1982.
- Lennartsson, W., R. D. Sharp, E. G. Shelley, R. G. Johnson, and H. Balsiger, Ion composition and energy distribution during 10 magnetic storms, *J. Geophys. Res.*, *86*, 4628-4638, 1981.
- McIlwain, C. E., Plasma Convection in the vicinity of the geosynchronous orbit, in *Earth's Magnetospheric Processes*, edited by B. M. McCormac, pp. 268-279, D. Reidel, Hingham, Mass., 1972.
- Rasmussen, C. E., S. M. Guiter, and S. G. Thomas, Two-dimensional model of the plasmasphere: Refilling time constants, *Planet. Space Sci.*, *41*, 35-43, 1993.
- Richards, P. G., and D. G. Torr, Seasonal, diurnal, and solar cyclical variations of the limiting H⁺ flux in the Earth's topside ionosphere, *J. Geophys. Res.*, *91*, 5261-5268, 1985.
- Roth, I., B. I. Cohen, and M. K. Hudson, Lower hybrid drift instability at the inner edge of the ring current, *J. Geophys. Res.*, *95*, 2325-2332, 1990.
- Shelley, E. G., D. M. Klumpar, W. K. Peterson, A. Ghielmetti, H. Balsiger, J. Geiss, and H. Rosenbauer, AMPTE/CCE observations of the plasma composition below 17 keV during the September 4, 1984 magnetic storm, *Geophys. Res. Lett.*, *12*, 321-324, 1985.
- Spjeldvik, W. N., Equilibrium structure of equatorially mirroring radiation belt protons, *J. Geophys. Res.*, *82*, 2801-2808, 1977.

Torr, M. R., D. G. Torr, P. G. Richards, and S. P. Yung, Mid- and low-latitude model of thermospheric emissions 1: $O^+(^2P)$ 7320 Å and $N_2(^2P)$ 3371 Å, *J. Geophys. Res.*, 95, 21,147-21,168, 1990.

Figure Captions

Figure 1. Time variations of (a) H^+ and (b) O^+ fluxes with initial energy peaking at 10 keV (top panel) and 40 keV (middle panel) in a background of thermal plasma (1 eV, density = 2000 cm^{-3}). The rate of energy loss as a function of ion energy is plotted in the bottom panel [taken from *Fok et al.*, 1993].

Plate 1. Upper panel: Model decay of Kp after the main phase of a moderate storm. Lower panels: 10-500 eV H^+ and O^+ fluxes in $cm^{-2} s^{-1}$ at different times during the recovery phase of the storm: (a) 0 hour, (b) 12 hours, and (c) 2 days [taken from *Fok et al.*, 1993].

Figure 2. Phase space distribution functions of ring current H^+ at 12 hours after the model moderate storm main phase. Dashed lines represent results when only drift is considered. Dotted lines contain effects of drift and charge exchange, while solid lines represent results under the same conditions except Coulomb collisions are also included.

Figure 3. Rate of energy change of ring current ions moving through a background thermal ion (1 eV H^+) gas as a function of the energy of the incoming ions.

Plate 2. Plasmaspheric ion volume heating rate at the equator (left) and the noon-midnight meridian (right) at (a) 2 hours and (b) 52 hours after the main phase of the model storm. The Kp values, for which the heating rates are shown, are indicated by red dots.

Figure 4. Simulated equatorial ion temperature for $L = 2$ (left) and $L = 4$ (right) as a function of time from the start of the storm recovery (RT = 0) and local time (LT). Results with and without heating from the ring current are shown in both panels.

Figure 5. Altitude profiles of ion temperatures for $L = 2$ (upper panel) and $L = 4$ (lower panel), morning (left) and evening(right) at different times relative to the start of the recovery. The temperature profile at $L=2$, 2200 LT for 66 hours RT falls on top of that with no ion heating. Mean DE 1/RIMS data in 1981 are shown with the \blacklozenge .

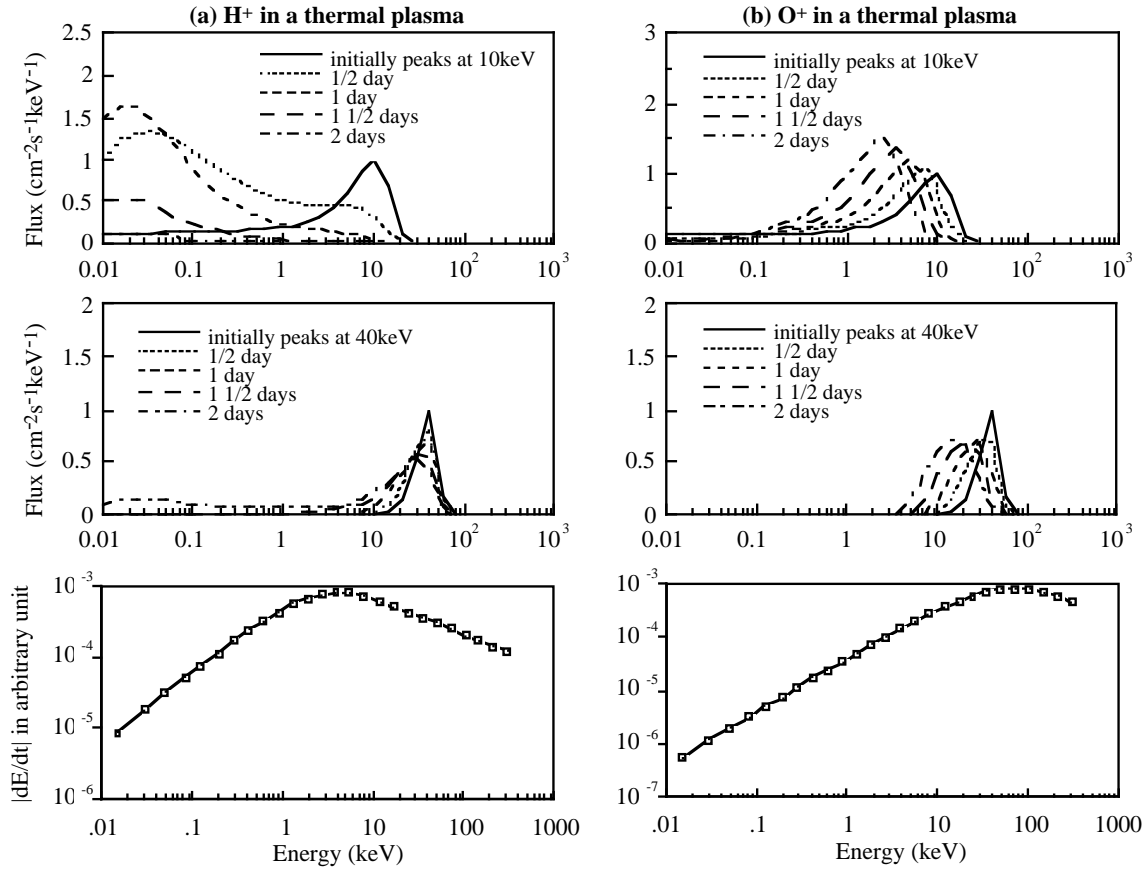
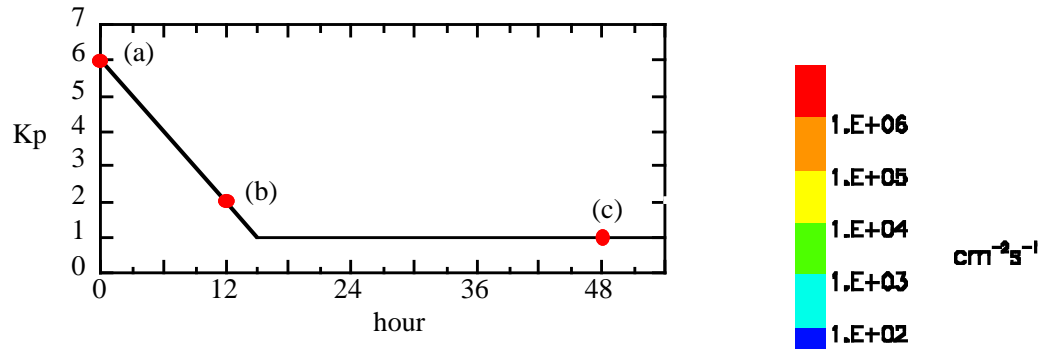
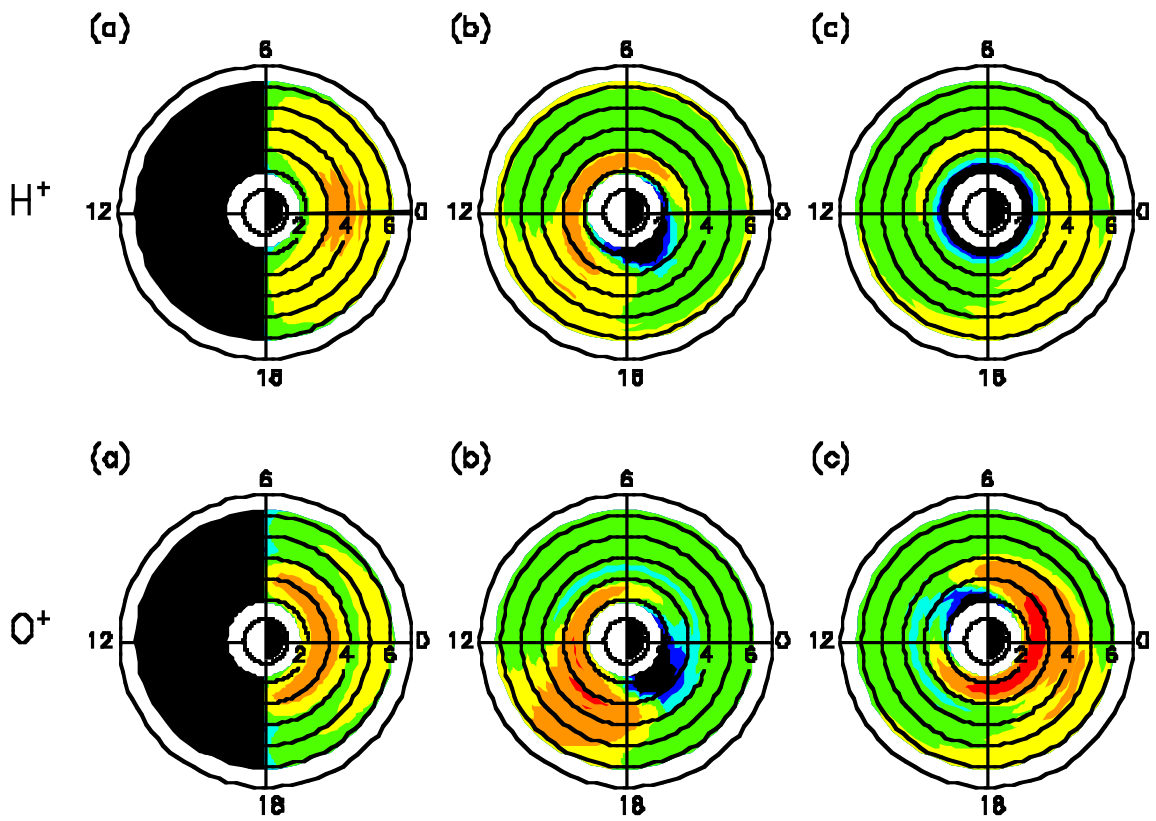


Figure 1



10 - 500 eV flux ($\text{cm}^{-2}\text{s}^{-1}$)



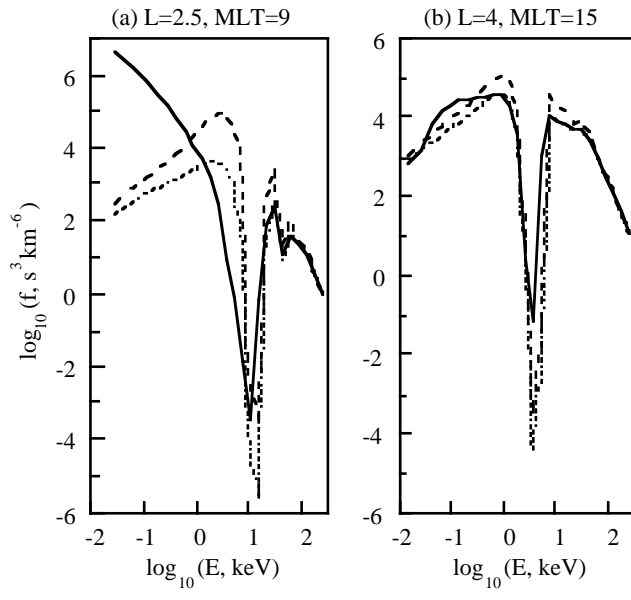


Figure 2

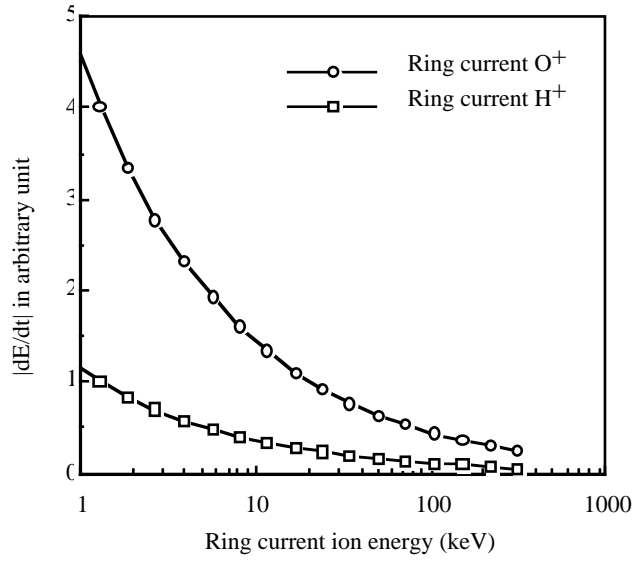
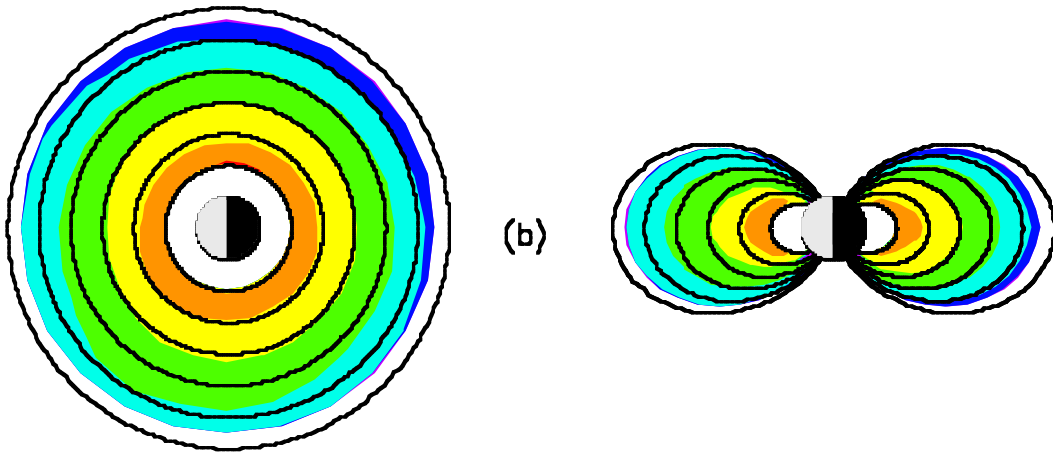
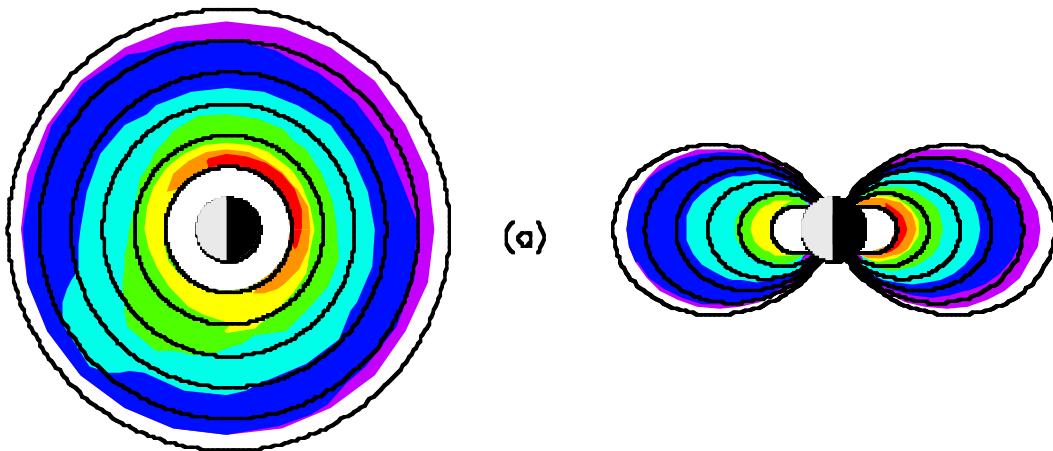
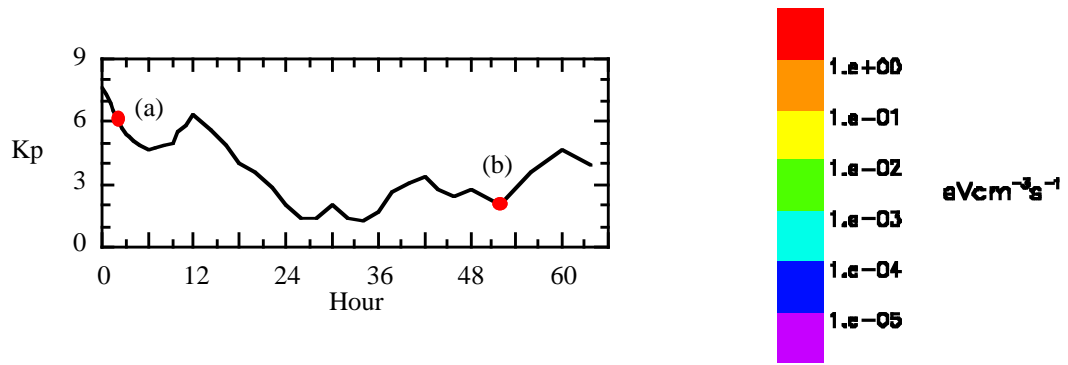


Figure 3



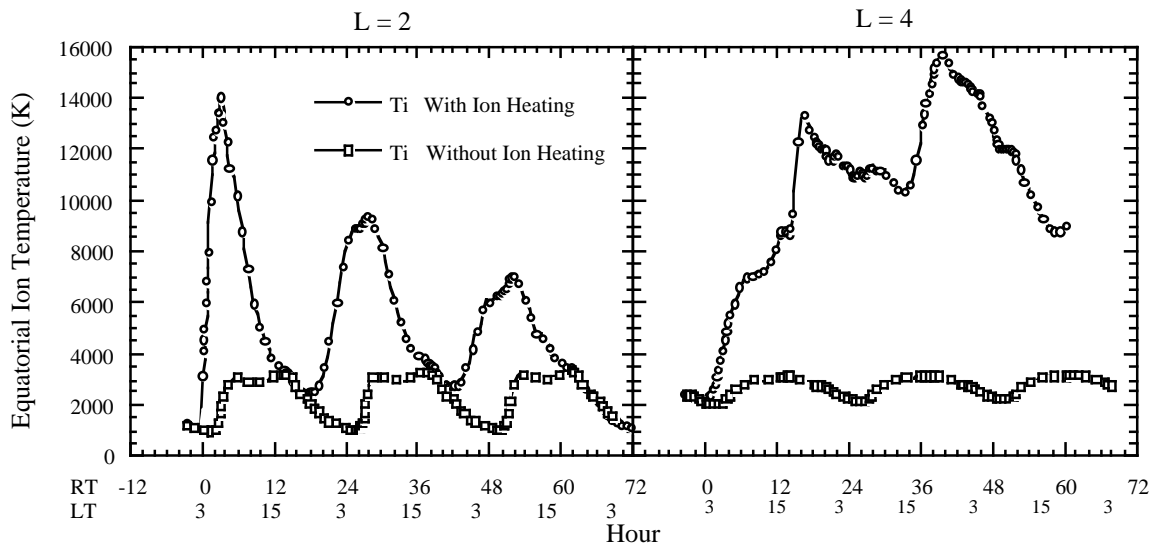


Figure 4

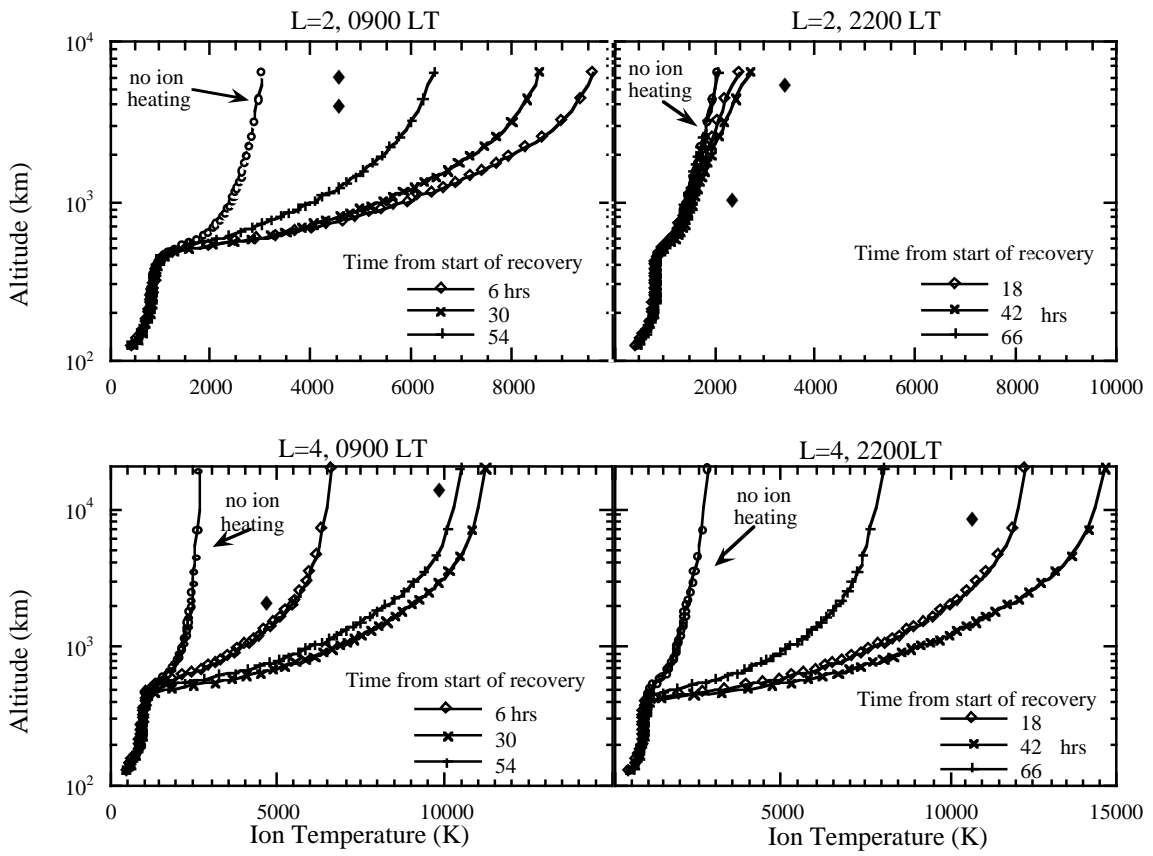


Figure 5